IEEE Access
Multidisciplinary : Rapid Review : Open Access Journal

Received June 2, 2019, accepted July 10, 2019, date of publication July 23, 2019, date of current version August 13, 2019.

Digital Object Identifier 10.1109/ACCESS.2019.2930534

Uniform Area Treatment for Surface Modification by Simple Atmospheric Pressure Plasma Treatment Technique

DONG HA KIM[1,2], CHOON-SANG PARK[1,3], BHUM JAE SHIN[4], (Member, IEEE), JEONG HYUN SEO[5], AND HEUNG-SIK TAE[1], (Senior Member, IEEE)

[1]School of Electronics Engineering, College of IT Engineering, Kyungpook National University, Daegu 702-701, South Korea
[2]Advanced Manufacturing Process Research and Development Group, Korea Institute of Industrial Technology, Ulsan 681-310, South Korea
[3]Digital Technology Research Center (DTRC), Kyungpook National University, Daegu 702-701, South Korea
[4]Department of Electronics Engineering, Sejong University, Seoul 143-747, South Korea
[5]Department of Electronics Engineering, Incheon National University, Incheon 406-772, South Korea

Corresponding author: Heung-Sik Tae (hstae@ee.knu.ac.kr)

This work was supported in part by the National Research Foundation of South Korea (NRF) Grant funded by the Korean Government (MOE) under Grant 2016R1D1A1B03933162, and in part by the Korean Government (MOE) under Grant 2018R1D1A1B07046640.

ABSTRACT The atmospheric pressure plasma jet (APPJ) has a merit to treat curved or 3D surface without using a ground electrode but nonetheless limits applications for expanding treatment area due to the localized ionization energy induced by the propagation along the direction of guided ionization waves. This paper proposes a uniform area treatment for surface modification based on the experimental case studies relative to variations of the APPJ structures, such as the number of array jets and guide-tube, including bluff-body (GB) system plus gas compositions. In these case studies, the current, infrared (IR), and optical emission spectrum (OES) are analyzed to investigate the factors affecting intensive glow-like plasma generation for uniform area treatment. Plasma-treated polyethylene terephtalate (PET) films are additionally examined to check the possibility of uniform area treatment for surface modification by using atomic force microscope (AFM), Fourier transform-infrared spectroscopy (FT-IR), X-ray photoelectron spectroscopy (XPS), and water contact angle (WCA). Only in case of three-array jets with GB system using Ar with O_2 gas, the intense glow-like plasma is observed to be produced widely in discharge space, thereby enabling the entire surface of PET films to be treated uniformly. In particular, the proposed APPJs are observed to generate more abundantly the reactive nitrogen species (RNS) ranging from 330 and 380 nm and the reactive oxygen species (ROS) at 777.4 and 844.6 nm. Furthermore, the plasma-treated PET film shows that the abundant RNS and ROS play a significant role in smoothening and changing its surface into hydrophilic surface. As a result, it is confirmed that the intense glow-like plasma generated broadly by the proposed APPJs can uniformly treat the entire surface of PET films.

INDEX TERMS Atmospheric-pressure plasmas, glow-like discharge, plasma diagnostics, polymer PET film, surface treatment.

I. INTRODUCTION

Recently, atmospheric pressure plasma (APP) device has attracted attention as advantages of non-thermal (low temperature), dry process, and replacing of conventional expensive low-pressure plasma. It has been applied to various fields, such as a surface modification [1], [2], polymer synthesis and deposition [3], [4], organic and inorganic materials etching [5], [6], and medical device [7], [8]. The surface modification and polymer synthesis using atmospheric pressure plasma jets (APPJs) and dielectric barrier discharge (DBD) have been extensively studied due to the advantage for localized three-dimensional (3D) treatments [9]–[12], and large area-treatments, respectively [13], [14]. The conventional APPJs have been known to be a promising growth source for a surface treatment because of the various benefits,

The associate editor coordinating the review of this manuscript and approving it for publication was Bora Onat.

such as low cost, simple structure, and treatment ability of curved surface without using a ground electrode [9]–[12]. Nonetheless, the plasma plume by the conventional APPJs has locally ionized energy due to its propagation along the direction of guided ionization waves or plasma bullet, thus resulting in limiting their applications for the uniformity of jet arrays and treatment effect [15]–[17]. Thus, for the uniform area-treatment process, less attention has been paid to APPJs than DBD technique. There has been a few attempts to apply the array jets with an increased number of jets to expanding the treatment-area, but the problem of localized treatment area still remains [16], [17]. The localized treatment area problem is inherently due to a streamer discharge produced in the conventional APPJs. To overcome this weakness of the conventional APPJs in view of a surface treatment, the required discharge characteristics would be a glow-like plasma instead of a streamer even though the jets are used as an APP source. In this sense, the new types of APPJs that can produce the intensified broad glow-like plasma in a discharge space needs to be studied. Our group has recently proposed a new plasma polymerization technique adopting an additional glass-tube and bluff-body (GB) system. As our previous works, we confirmed that the secondary flow and static pressure were increased via optimized GB system [18], meaning that the flow direction of the plasma produced by the APPJs was randomly changed against the flow direction of gas in which it normally appeared in the conventional APPJs. Accordingly, the guided ionization waves were weakened and converted into an intense glow-like plasma due to the randomness of gas flow direction with the help of GB system in the APPJs [18].

The aim of this study is to improve the surface area treatment capability of the conventional APPJs by carrying out the case studies depending on the variations of APPJ structure, such as the number of array jets and guide tube including bluff-body (GB) system plus gas compositions.

In this study, we have examined single, three, and seven array-jets structures to investigate the effects of the GB system on the expansion of the array jets. The current, IR and optical emission spectrum (OES) were monitored to examine which are the significant factors affecting the intense glow-like plasma generation for uniform area-treatment. Our experimental results will show that the uniform and intense glow-like plasma can be produced only in case of three-array jet with GB system using Ar with O_2 gas. In addition, the reactive nitrogen species (RNS) of second positive system (SPS) and reactive oxygen species (ROS) have increased drastically because the Ar discharge gas stays longer and frequently interacts with the intense plasma in discharge region via GB system.

Plasma-treated flexible PET films were also analyzed to investigate the influence on surface modification by the intense glow-like plasma for uniform area-treatment. Atomic force microscope (AFM) was measured in center region of the films to confirm the smoothness of the plasma-treated surface due to the significant increase in the RNS.

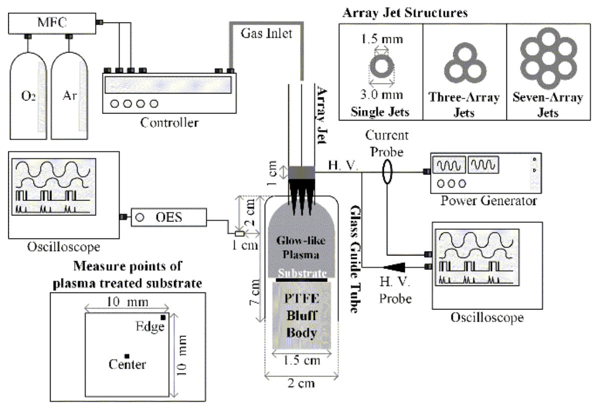

FIGURE 1. Schematic diagram of experimental setup in this study.

Fourier transform-infrared spectroscopy (FT-IR), and X-ray photoelectron spectroscopy (XPS) were measured in center and edge regions of the films to check chemical bond changes. Water contact angle (WCA) was measured in several regions of the films to investigate the hydrophilic surface of the entire plasma-treated film in view of uniform area-treatment. As a result, plasma-treated PET films show that the RNS and ROS play an important role in surface smoothing and helping a hydrophilic surface. In addition, the plasma produced by the GB system uniformly treated the entire surface of the PET film, confirming that there exist a clear correlation among the plasma pattern formation, surface wettability, surface chemistry, and morphology.

II. METHOD

A. ATMOSPHERIC PRESSURE PLASMA JETS (APPJS) WITH GUIDE-TUBE AND BLUFF-BODY (GB) SYSTEM

Fig. 1 shows a schematic diagram of the experimental setup used in this study. A plasma jet tube with an inner diameter of 1.5 mm and an outer diameter of 3 mm was 130 mm long and connected to the power generator by copper tape having a width of 10 mm from the end of the tube. The GB system consisted of a glass guide-tube and a polytetrafluoroethylene (PTFE) bluff-body. The guide-tube had a length of 60 mm and an inner diameter of 20 mm, whereas the bluff-body had an outer diameter of 15 mm. It should be emphasized that the glass guide-tube is adopted to induce further vigorous secondary flow and static pressure of discharge gases, which is one of the critical components of the proposed APPJ. This GB system spread the plasma in the discharge region [18]. Thus, three array jet structures were prepared to increase the treatment-area, as shown in Fig. 1. The high purity Ar/He (99.999 %) with O_2 (99.999 %) gases were used and flow rates were 3000 and 15 standard cubic centimeters per minute (sccm) in all cases, respectively.

A sinusoidal voltage with a peak value of 10 kV and a frequency of 30 kHz was applied to the powered electrode. The PTFE bluff-body in the GB system acted as a floating electrode. A voltage probe (Tektronix P6015A), current monitor

(Pearson 4100) and oscilloscope (LeCroy WaveRunner 64Xi) were used to measure the sinusoidal voltage and current.

B. PLASMA DISCHARGE ANALYSES

The photo-sensor amplifier and OES techniques were used to analyze the optical intensity and spectra of reactive nitrogen and oxygen peaks, respectively. The photo-sensor amplifier (Hamamatsu C6386-01) was used to measure infrared (IR) emissions in the discharge region. An optical emission spectrometer (OES, Ocean Optics, USB-4000UV-VIS) was employed to monitor the nitrogen and oxygen reactive radicals in plasma. As shown in Fig. 1, the optical fiber of the optical emission spectrometer (OES) was positioned at a distance of 1 cm away from the guide-tube for horizontal location and 2 cm below the top of guide-tube for vertical location. The position of the optical fiber for measuring the IR emission was exactly the same as that of the OES.

All photographs of plasma plumes were taken with a DSLR camera (Nikon D5300) with a Macro 1:1 lens (Tamron SP AF 90mm F2.8 Di).

C. ANALYSES OF PLASMA-TREATED PET FILM

The flexible polyethylene terephtalate (PET) film was used as a substrate for plasma treatment and ultrasonically cleaned in 99.99% isopropanol and distilled water for 20 min, respectively, to remove contamination on the surface of the PET film. All the plasma-treated samples were measured and analyzed three times. AFM (Park Systems NX20) was used to monitor the surface roughness of PET films with a scanning area of 3 $\times$ 3 μm. The effects of the proposed APPJs on smoothness of surface morphology of plasma-treated PET film are examined by the AFM measurement. The AFM measurement point is specified in the center region of the plasma-treated PET film. The FT-IR and XPS analyses were used to determine the surface chemical changes of PET film treated by plasma. The FT-IR was taken using a Perkin-Elmer Frontier spectrometer between 650 and 4000 cm^{-1}. XPS was carried out using an ESCALAB 250Xi surface analysis system (Thermo Fisher Scientific, Waltham, MA, USA) with a monochromatic Al Kα X-ray source (hυ = 1486.71 eV) operated at 15 kV and 20 mA. The WCA analysis (DSA100m, Kruess) was conducted by the static sessile drop method and measured using a drop shape analysis system, consisting of a piezo dosing head which can dispense drops as small as 40 mL. The specified location of measurements for the plasma-treated PET films is depicted in Fig. 1.

III. RESULTS AND DISCUSSION

A. OPTICAL AND ELECTRICAL DISCHARGE CHARACTERISTICS OF PLASMA

In order to get better understandings of the key factors, affecting glow-like plasma generation for uniform area-treatment, several parameter studies, in terms of device structures, such as the number of array jets, cases of employed GB systems (proposed APPJ) or not (conventional APPJ), were conducted and analyzed over time.

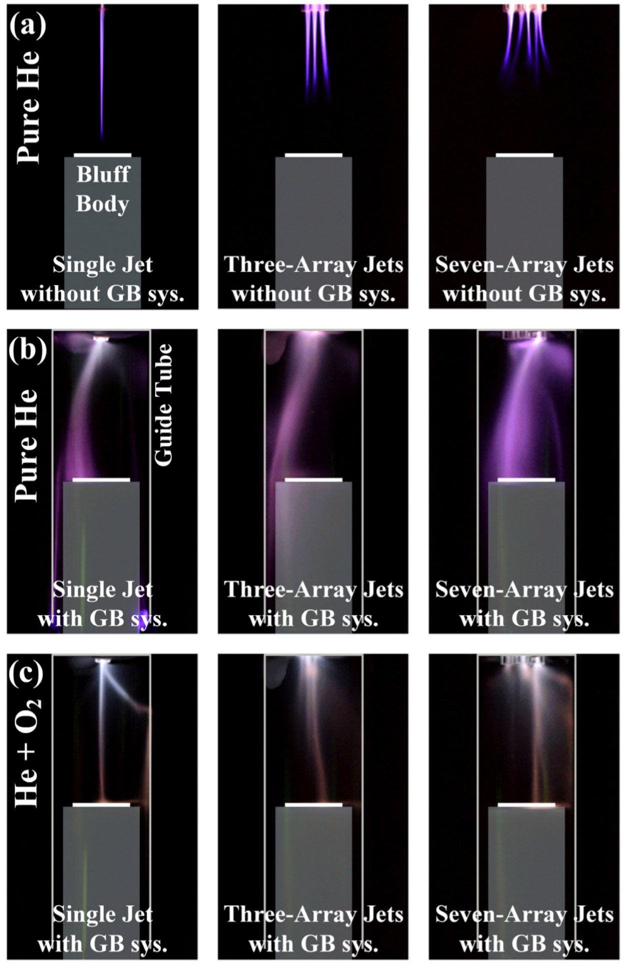

FIGURE 2. Plasma images: (a) pure He plasma without GB system, (b) pure He plasma with GB system, and (c) He + O_2 plasma with GB system relative to number of array jets (single jet, three-array jets, and seven-array jets) for uniform area-treatment.

1) PLASMA IMAGES

Fig. 2 (a) shows the plasma images relative to the number of jet arrays in the case of pure He gas when the GB system is not employed. In general, it is not difficult to generate the He plasma at the APPJ due to the low discharge voltage characteristic. In addition, since the He has a high mobility and as such He plasma has a long life-time characteristic, the He plasma can be formed stably even when the number of the jet arrays is expanded to three or seven. However, for the pure He case, simply extending the number of array jets did not enable a uniform production in a large area because individual plumes were formed independently, as shown in Fig. 2 (a).

Fig. 2 (b) shows the plasma images relative to the number of jet arrays in the case of pure He gas when the GB system is employed. As shown in Fig. 2 (b), the He plasma was diffused in the guide-tube, but it was formed unstably as a whole, implying that the pure He plasma was not suitable for large area treatment even though the number of array jets was increased under the GB system.

The addition of a small amount of O_2 gas is known to be reported to be effective to keep plasma from changing arc

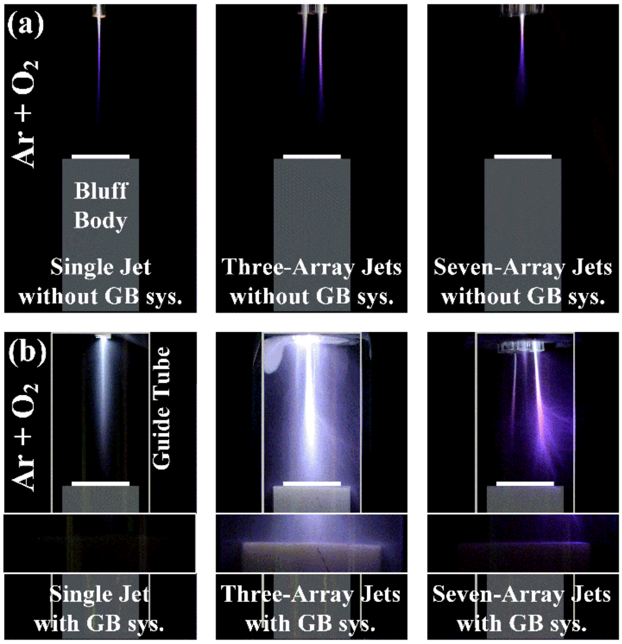

FIGURE 3. Plasma images: (a) Ar with O_2 plasma without GB system and (b) Ar with O_2 plasma with GB system relative to the number of array jets (single jet, three-array jets, and seven-array jets, respectively) for uniform area-treatment.

discharge as an electronegative gas [19], [20]. Thus, an additional experiment was carried out to investigate the influence of O_2 gas on the diffusion of the He plasma under various array jets. As shown in Fig. 2 (c), nonetheless, the propagation of a plasma plume was difficult to control due to the properties of a longer plume corresponding to the high drift velocity caused by the lower mass and high metastable energy of the He atoms, resulting in the still localized plasma irrespective of adding an O_2 gas [21]–[23].

For the pure Ar plasma, the Ar plasma tended to be produced very unstably irrespective of adopting the GB system (not shown here). It is known that since Ar atoms have a lower metastable energy (11.6 eV), the Ar plasma plume has to proceed via the streamer discharge to generate filamentous plasma due to the lower penning ionization rate [21], [22].

Moreover, the lower ionization energy (15.8 eV) would affect the production of abundant ions and electrons and as such lead to glow-to-arc transition [24]. As a consequence, the Ar + O_2 plasma instead of pure Ar plasma was examined in this experiment.

Fig. 3 (a) shows the Ar + O_2 plasma images relative to the number of array jets without GB system. When a small amount of O_2 gas was added into Ar gas, the arc transition was alleviated by O_2 gas as an electronegative gas, compared to using only Ar gas (not shown here). However, the Ar plasma plumes emitted from the array jets were not interacted mutually and merged into intense glow-like plasma for uniform-area treatment even though the number of array jets were increased up to seven, as shown in Fig. 3 (a). As shown in Fig. 3 (b), in the case of adopting the GB system, the stable glow-like plasma was produced due to the combined effects of O_2 gas (*i.e.*, suppression of glow-to-arc transition) and GB system (*i.e.*, transition of guided ionization wave to glow-like plasma) [18].

Our previous simulation result [18] on the gas flow mechanics about the guide-tube and bluff-body system has shown that the impinging gas flows on the bluff-body were mixed with the incoming gas flow from upstream, thereby producing an intense and broadened plasma near the bluff-body.

This simulation results are still applicable to our present experiment because the vaporized monomer is simply replaced by the electronegative gas such as oxygen gas. Similar results were also reported by Knoll et al. and Zhu et al. for changing from plasma bullets patterns to diffusive plasma patterns in enclosed environment matching feed gas chemistry using Ar and He APPJs, respectively [25], [26].

For seven-array jets, intense repulsion-force would work at the center jet and as such the other Ar plasma plumes become weak, thereby inducing unstable plasma [27]. Furthermore, our experiment adopted a floating electrode instead of a ground electrode, which would cause a plasma production for each jet more difficult, as shown in Fig. 3 (b) [27], [28].

On the other hand, in case of three-array jets with GB system, the intense and broadened glow-like plasma, especially at the vicinity of the surface of bluff-body where the PET films were placed, was produced, as shown in the magnified image of Fig. 3 (b).This intense and broadened glow-like plasma was very similar to that in our previous result [18]. On the other hand, in case of seven array jets with GB system, the streamer-like discharge was observed only in the localized area especially at the right side, as shown in the magnified image of Fig. 3 (b). A repulsion-force did not work only at a specific part of the device since the structures of the three glass tubes were completely symmetrical from a geometrical point. As a result, all three plumes were independently generated and came out at the edge of the glass tube and all three plumes could interact and merge into an intense glow-like plasma, as shown in Fig. 3 (b). Thus, these results support that the unique features, such as 1) origin characteristics of Ar atoms (lower ionized and metastable energies) and 2) increase of secondary flow and static pressure with the help of GB system, influenced the generation of abundant ions and electrons, and diffusion in Ar discharge channel effectively. In addition, it is also notable that the Ar plasma behavior was not transited to arc discharge because of O_2 effect and showed diffusive and glow-like discharge, covering the entire surface of the film uniformly. Based on these results, we have focused 1) on the study of plasma discharge to single-jet, and three-array jet cases, and 2) on the study of effects of adopting the GB system, in terms of expandability on uniform area-treatment.

2) CURRENT AND IR ANALYSES

Fig. 4 shows the applied voltages, total currents, and IR emission intensities of Ar with O_2 plasma without/with GB system relative to the number of array jets for uniform

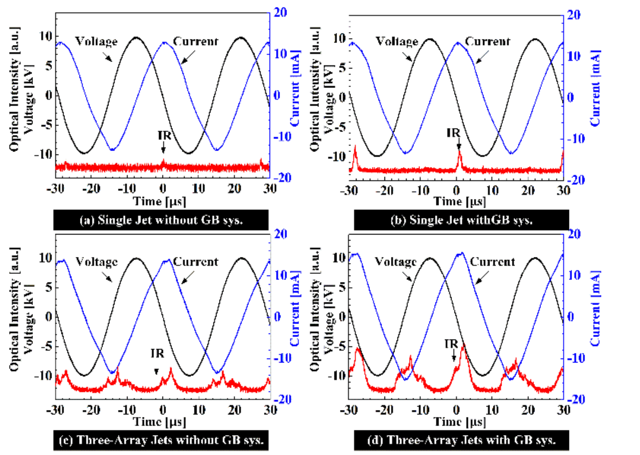

FIGURE 4. Applied voltages, total currents, and IR emission intensities of Ar with O_2 plasma: (a) single jet without GB system, (b) single jet with GB system, (c) three-array jets without GB system and (d) three-array jets with GB system.

area-treatment. As shown in Fig. 4 (b) and (d), the current and optical intensities increased significantly, even when the same voltages and gas flows were applied, implying a high plasma energy state. It is presumably due to the enclosed environment that the Ar discharge gas was confined longer in a discharge region and then excited and ionized by plasma more frequently with the help of GB system as shown in our previous work [18].

3) OES ANALYSIS

The reactive nitrogen species (RNS) and reactive oxygen species (ROS) are known to play an important role in surface modification for hydrophilic property of biological/medical applications [29], [30]. To investigate the mechanism of intense glow-like plasma generation and effect of the GB system on the reactive radical species produced by the Ar with O_2 plasma, the optical emission spectra were measured in the single and three-array jets without/with GB system, respectively, as shown in Figs. 5 (a) and (b). The RNS peaks of second positive system (SPS) are related to the wavelength ranging from 330 to 381 nm, whereas the ROS peaks are related to the wavelengths at 777.4 and 844.6 nm. The excited Ar radicals are related to the wavelength ranging from 695 to 850 nm. When adopting the GB system, the peaks of excited N_2 SPS were observed to be increased. In particular, at the three-array jet condition, the peak of excited N_2 SPS was increased considerably. In addition, in order to analyze ROS peaks, the measured OES was magnified in the wavelengths ranging from 760 to 865 nm, as shown in Fig. 5 (b). When the GB system was adopted, the ROS peak of 777.4 nm was also significantly increased and the ROS peak of 844.6 nm was newly observed.

The role of GB system is to minimize the quenching from ambient air and simultaneously confining the jet flow in the discharge region by reducing an exhaust gas flow. In case of APPJs with GB system, the secondary flow and resultant recirculation flow motion are created due to the

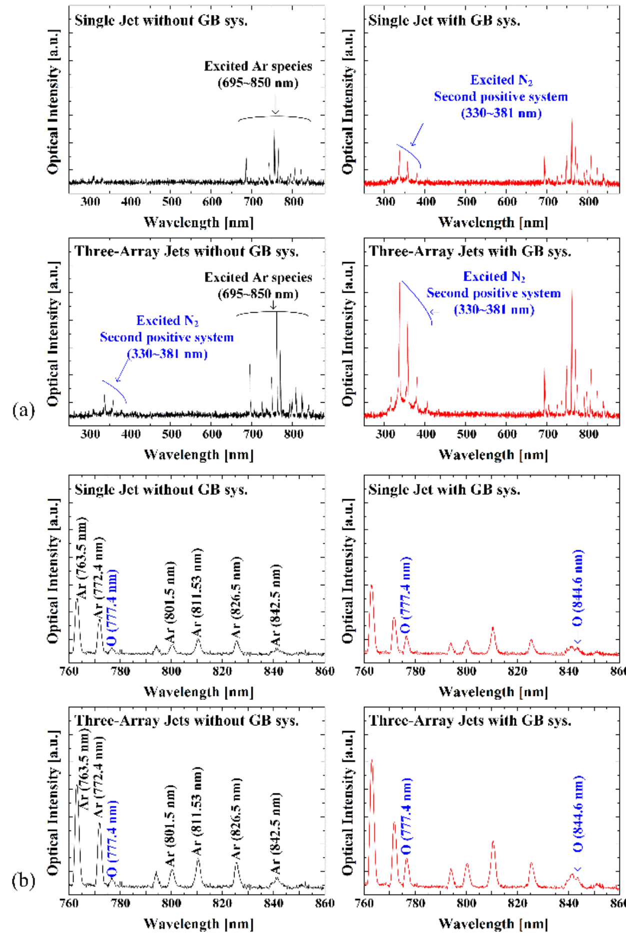

FIGURE 5. OES from Ar + O_2 plasma in wavelength ranging (a) from 250 to 880 nm, and (b) from 760 to 860 nm in single or three-array jets without/with GB system.

guide-tube and bluff-body, thereby enhancing the mixing condition between the Ar gas stream near the bluff-body and newly incoming Ar gas flows. Consequently, intensified glow-like plasma is produced in the vicinity of the bluff-body [18]. In this case, the high Ar plasma energy can be transferred to the RNS and ROS in a discharge region through a plasma coupling or plasma interaction of the plasma plume produced from the several jets at a specific discharge condition especially in the presence of the GB system [31]. In particular, the N_2 species requiring a higher breakdown voltage are the most actively excited than any other ambient species [32].

As shown in Figs. 5 (a) and (b), for APPJs with GB system, the sharply increased intense peaks of excited N_2 SPS and O_2 were observed in comparison with the intense peaks of Ar. This OES result of Fig. 5 (a) confirms that even though the amount of N_2 species participating in the discharge from the ambient air is minimized, the N_2SPS can further decomposed and activated thanks to the presence of the GB system in the APPJs.

To compare the OES analysis quantitatively among the excited species, the emission intensities of single jet without

TABLE 1. Normalized intensities of Ar with O_2 plasma in single or three-array jets without/with GB system.

Samples	N_2 SPS 337.1 [nm]	Ar 678.1 [nm]	O 777.4 [nm]	O 844.6 [nm]
Single jet without GB system	1	1	1	-
Single jet with GB system	4.2	1.1	3.0	New
Three-array jets without GB system	2.3	1.5	1.1	-
Three-array jets with GB system	13.9	1.8	3.8	New

GB system are normalized as reference emission intensities. For comparison, other emission intensities are divided by the reference emission intensities. The detailed values are summarized in Table1. As shown in Table 1, in the three-array jets with GB system, the normalized peak of N_2 SPS at 337.1 nm was increased almost 14 times more intense than in the single jet without GB system. In the three-array jets with GB system, the normalized peak of O at 777.4 nm was increased almost 4 times more intense than in the single jet without GB system. On the other hand, in the three-array jets with GB system, the normalized peak of Ar at 678.1 nm was increased about 1.8 times more intense than in the single jet without GB system.

B. CHARACTERIZATION OF PLASMA-TREATED PET FILM

In order to verify the effects on PET Films treated by the intense glow-like plasma in this experiment, we investigated the characteristics of the plasma-treated PET films such as surface morphology, chemical compositions, and associated hydrophilicity features. In particular, to get better understandings of the effects of intense glow-like plasma on uniform area treatment, the chemical compositions of the plasma-treated films with hydrophilic surface features were analyzed by the FT-IR, XPS, and WCA analyses at several positions of the films.

1) AFM ANALYSIS

In AFM measurement, the effects of significant increase of N_2 SPS on the surface morphology were examined. Fig. 6 shows the images of AFM measured in the center region of plasma-treated PET films via Ar with O_2 plasma after 10 sec in the single or three-array jets without/with GB system. The morphology of the pristine PET film was quite smooth, with an average root mean square roughness (Rrms) value of 0.443 nm, determined in a 3 μm × 3 μm surface of the film. As shown in Fig. 6, the considerable topographical changes were observed after plasma treatment without the GB system. The AFM results exhibited that the particle-like irregular protuberances and blisters were generated, and the roughness was increased substantially, compared to pristine PET from 0.443 to 9.714 nm. These results are in agreement with the trend observed by Fang *et al.* [33] and Novák *et al.* [34]. Without GB system, the surface roughness of plasma-treated PET film was observed to be increased irrespective of the number of array jets, single, three, and seven (not shown here).

On the other hand, when the PET film was treated by the intense glow-like plasma produced by the GB system,

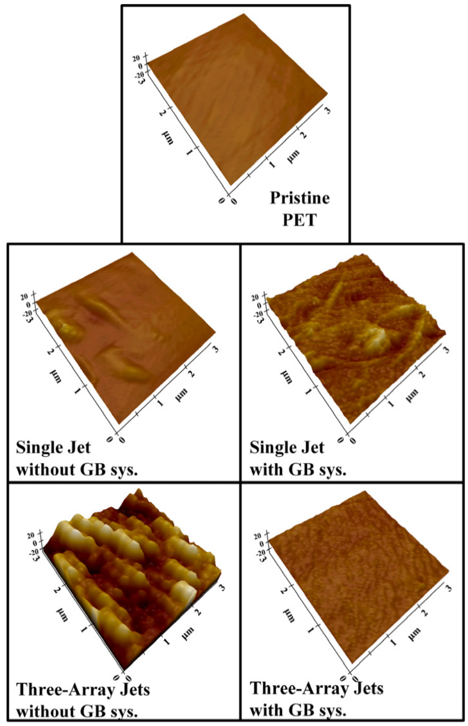

FIGURE 6. AFM images of pristine and plasma-treated PET film via Ar with O_2 plasma after 10 sec in single or three-array jets without/with GB system.

TABLE 2. Calculated Ra and Rrms of pristine and plasma-treated PET film via Ar with O_2 plasma after 10 sec in single or three-array jets without/with GB system.

Samples	Ra [nm]	Rrms [nm]
Pristine PET	0.357 ± 0.281	0.443 ± 0.321
Single jet without GB system	1.051 ± 0.842	1.536 ± 0.922
Single jet with GB system	2.902 ± 1.021	3.919 ± 1.252
Three-array jets without GB system	7.904 ± 2.073	9.714 ± 2.311
Three-array jets with GB system	0.923 ± 0.384	1.172 ± 0.422

the surface of the PET film was changed into a smooth one, as shown in the AFM image of three-array jets with GB system in Fig. 6. For the single and seven (not shown here) array jets, the surfaces roughness of plasma-treated PET film was still increased even though the GB system was adopted.

The detailed data of average surface roughness (Ra) and Rrms with deviations are summarized in Table 2. It would be inferred that the abundant excited N_2 radicals could be produced by the intense glow-like plasma with the help of GB system, thus contributing to smoothing the surface of the

TABLE 3. Elemental compositions of pristine and plasma-treated PET film via Ar with O_2 plasma after 10 sec in three-array jets without/with GB system.

Samples	Atomic percent [at%]		
	C	O	N
Pristine PET	74.4 ± 3.1	25.6 ± 2.7	-
Three-array jets without GB system at center	69.0 ± 2.6	31.0 ± 1.9	-
Three-array jets without GB system at edge	68.2 ± 3.7	31.8 ± 2.8	-
Three-array jets with GB system at center	58.0 ± 1.8	39.0 ± 1.2	3.0 ± 0.1
Three-array jets with GB system at edge	61.0 ± 2.1	36.3 ± 1.6	2.7 ± 0.3

PET film [35]. Through AFM measurement, the changes in the surface morphology of the plasma-treated PET film were monitored, confirming that the most smooth surface of the PET film was obtained by the treatment of the plasma produce by the three-array jet with GB system. With the changes in the surface morphology of the plasma-treated PET film, another surface characteristics such as, chemical bonds and hydrophilicity of the plasma-treated PET films were simultaneously examined by the XPS and WCA measurements, respectively. In addition, these results are expected to be applied to research fields requiring very smooth thin films less than 10 nm, such as a conducting electrode layer of polymer light emitting diode (P-LED) device [18].

2) FT-IR ANALYSIS

In order to confirm the uniformity of the area-treatment by the proposed APPJs, *i.e.*, three-array jets with GB system, the bonding structures of the plasma-treated PET surface were analyzed in the center and edge regions, respectively, as shown in Fig. 1. Fig. 7 (a)-(d) show the FT-IR images of the pristine and the PET film treated for 10 sec using Ar with O_2 plasma in wavenumber ranging from 650 to 4000 nm. As shown in Fig. 7 (a) and (c), *i.e.*, conventional APPJ without GB system, the variation of the chemical bond of the plasma-treated PET film was more significant at the center point compared to the chemical bond at the edge point. It is attributed to the localized processing area due to the guided streamer typically observed in conventional APPJ [12].

On the other hand, as shown in Fig. 7 (d), *i.e.*, proposed APPJs, three-array jets with GB system, the bonding structure between the center and edge points was subsequently identical. Comparing Figs. 7 (a) and (c) (single, three, and seven (not shown here) array jets without GB system) to Figs. 7 (b) and (d) (single, three, and seven (not shown here) array jets with GB system), when the GB system was adopted, the peaks between 700 and 2000 cm^{-1} were decreased significantly, whereas the peaks between 2000 to 3500 cm^{-1} were increased broadly. It is presumably due to the -NH stretching band between 3300 and 3340 cm^{-1}, or OH stretching vibrations between 3300 and 3650 cm^{-1} [36], [37]. In addition, we also observed the increase of C-O peak of oxygen bonding at 2100 cm^{-1} and nitrogen bonding at 2350 cm^{-1} [37], [38]. Consequently, the uniformity of the area-treatment by the proposed APPJs, three-array jets with GB system was confirmed by showing the coincidence of the peaks of FT-IR between the center and edge regions of the plasma-treated PET films. The main bonding structures for the hydrophilic surface are further examined in detail by the XPS measurement.

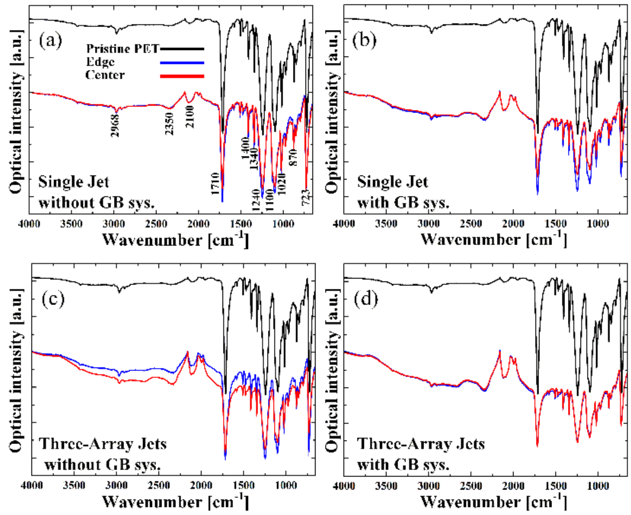

FIGURE 7. FT-IR images in wave number ranging from 650 to 4000 nm of plasma-treated PET films via Ar with O_2 plasma for 10 sec: (a) single jet without GB system, (b) single jet with GB system, (c) three-array jets without GB system, and (d) three-array jets with GB system. Pristine PET is used as reference.

3) XPS ANALYSIS

Figs 8 (a) and (b) show the bar-plots presenting (a) the atomic concentration ratio and (b) the deconvoluted C1s core level spectra measured in the center and edge regions of the plasma-treated PET film using an Ar with O_2 plasma for 10 sec in the proposed APPJs, *i.e.*, the three-array jets with GB system, respectively. For comparison, the pristine PET film was also measured in the center region, as shown Figs. (8) and (b). As shown in Fig. 8 (a), the oxygen content was increased, whereas the carbon content was decreased when the GB system was adopted [39], [40]. It should be noted that the nitrogen content was newly detected, which was not detected in case of the conventional APPJs. This new detection of nitrogen content in the plasma-treated PET film is presumably due to the significant increase of N_2 SPS induced by the proposed APPJs system with GB system, as already shown in the OES data of Fig. 5 (a).

The decomposition of C1s peak is related to the carbon bonding with oxygen in polymer surface modification caused

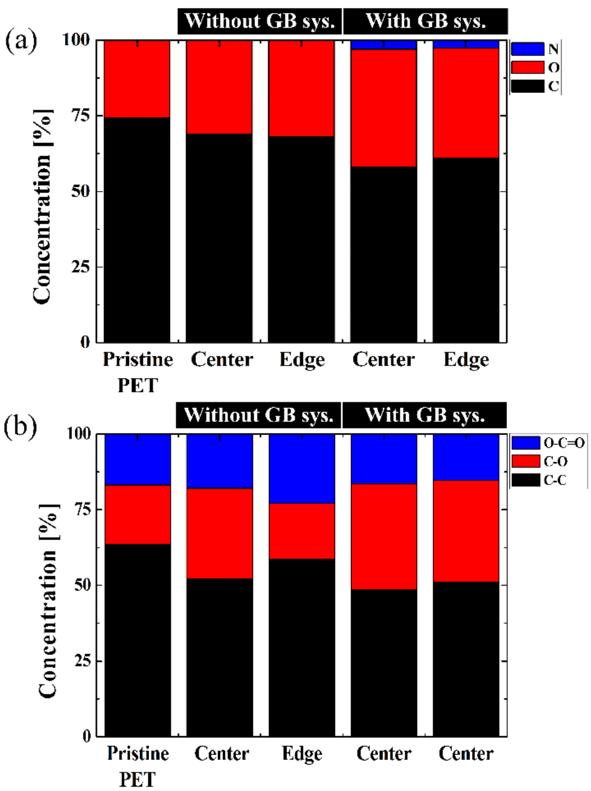

FIGURE 8. Bar-plots presenting (a) atomic concentration ratio and (b) deconvoluted C1s core level spectra measured in center and edge regions of plasma-treated PET films via Ar with O_2 plasma for 10 sec in three-array jets without/with GB system. In pristine PET film, center region is measured.

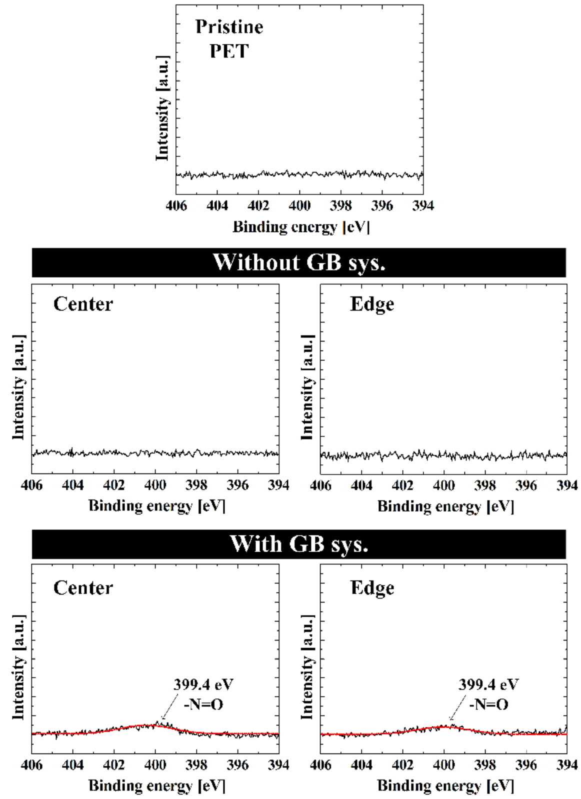

FIGURE 9. Deconvoluted N1s core level spectra of pristine and plasma-treated PET film via Ar with O_2 plasma for 10 sec at center and edge points in three-array jets without/with GB system.

by plasma. The concentration of C1s spectra was calculated by deconvolution using Lorentzian fit and its result was shown in Fig. 8 (b). C1s peak was deconvoluted into three peaks: 1) a peak of 284.6 eV by C-C/C-H bonds (C1); 2) a peak of 286.2 eV by C-O/C-OH bonds (C2); and 3) a peak of 288.6 eV by O=C-O/C-OOH bonds (C3). As shown in Fig. 8 (b), when the GB system was adopted, the peak at 284.6 eV (C1) was observed to be decreased, while the oxygen-containing hydrophilic polar groups, such as C–O/C-OH bonds (C2), were increased, thus affecting the resultant hydrophilic capability of the PET surface. Furthermore, chemical bonding properties at the center and edge points of PET films were well coincided.

On the other hand, in the case of the PET surface treated by plasma without GB system, the similar bond as pristine PET was observed at edge point [41], as shown in Fig. 8 (b), indicating that conventional APPJ treated the PET surface only locally, as confirmed by FT-IR analysis shown in Fig. 6. Based on the XPS data of Figs. 8 (a) and (b), the changes in the elemental compositions and relative chemical compositions of C1s and N1s spectra are summarized in Tables 3 and 4, respectively.

Meanwhile, as shown in Fig. 9, when the GB system was adopted, the nitrogen chemical bonding of 399.4 eV ascribed to -N=O bond was newly observed in comparison with that in case without GB system [34]–[37]. These results are deeply related to the production of abundant N_2 SPS with high reactivity induced by the intense glow-like plasma of the proposed APPJs with GB system. The surface of PET film was so exposed to the discharge space with abundant N_2 SPS that it reacted with the activated nitrogen species during plasma treatment process, thereby resulting in observing the nitrogen chemical bonding by the XPS. The -N=O bond detected in the PET film confirms the hydrophilic feature of the plasma-treated PET films [36], [37].

In conclusion, the abundant N_2 SPS by the intense plasma contributed to modifying the PET film surface to become more smooth and hydrophilic with the help of GB system. Furthermore, the broadened and intense glow-like plasma with RNS and ROS produced with the help of GB system, enabled the entire surface of PET films to be treated uniformly.

4) WCA ANALYSIS

In order to confirm the uniform surface treatment with hydrophilicity by the proposed APPJ, *i.e.*, three-array jets with GB system, WCA measurement was performed for 16 regions by dividing the entire area (=10 mm × 10 mm) of PET substrate into 2.5 mm intervals, as shown in Fig.10 (a).

Figs. 10 (b) and (c) show the 2D graphs of WCA of PET films treated with Ar + O_2 plasma for 10 sec for the entire area [11], [40].

TABLE 4. Relative chemical compositions of C1s and N1s spectra of pristine and plasma-treated PET film via Ar with O_2 plasma after 10 sec in three-array jets without/with GB system.

Samples	Atomic percent [Area%]			
	C-C/C-H 284.6 eV	C-O/C-OH 286.2 eV	O-C=O 288.6 eV	-N=O 399.4 eV
Pristine PET	63.4 ± 3.9	19.8 ± 2.1	16.8 ± 1.1	-
Three-array jets without GB system at center	52.1 ± 2.8	30.0 ± 1.9	21.9 ± 0.6	-
Three-array jets without GB system at edge	58.7 ± 4.3	18.4 ± 3.3	22.9 ± 0.5	-
Three-array jets with GB system at center	48.5 ± 2.5	35.0 ± 2.0	16.5 ± 0.2	New
Three-array jets with GB system at edge	51.0 ± 2.7	33.7 ± 1.8	15.3 ± 0.6	New

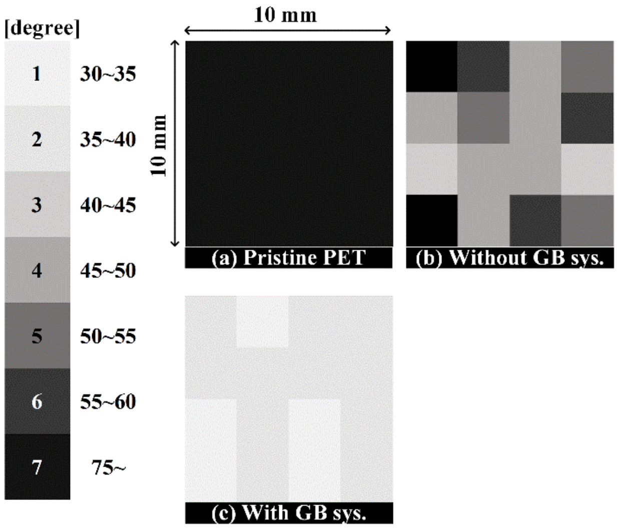

FIGURE 10. 2D graphs of WCA of (a) pristine PET film and plasma-treated PET film via Ar with O_2 plasma for 10 sec at 16 points in three-array jets (b) without and (c) with GB system for uniform area-treatment.

Table 5 shows the calculated contact angle average (CAa) and contact angle standard deviation (CAsd) obtained from the measured WCA values of Fig. 10. As shown in Fig. 10 (b), when the GB system was not adopted, the WCA values were in the wide range of 40 and 75°, and especially the edges of the PET substrate were not treated well by the plasma. The oxygen atom content and the C-O/C-OH bond at the edge point are considered to have been observed to be lower than the center point.

On the other hand, when the GB system is adopted, all the WCA values were obtained between 30 to 40°, as shown in Fig. 10 (c), meaning that the hydrophilic surface treatment was effectively performed by the intense glow-like plasma generated by the three-array jets with GB system. It is notable that the very low CAsd (=2.8°) in the three-array jets with GB system confirms a successful realization of uniform surface treatment, as shown in Table 5.

In addition, in the proposed APPJs, *i.e.*, three-array jets with GB system, the higher oxygen-containing hydrophilic polar groups, such as C-O/C-OH bonds at both the center and edge points, are in good agreement with the XPS measurements with high oxygen atom content. Therefore, it can be inferred that uniform surface treatment for the PET substrate

TABLE 5. Calculated CAa and CAsd of pristine and plasma-treated PET film via Ar with O_2 plasma after 10 sec in three-array jets without/with GB system.

Samples	CAa [degree]	CAsd [degree]
Pristine PET	77	-
Three-array jets without GB system	53.1	10.5
Three-array jets with GB system	35.4	2.8

is highly dependent on the plasma generation pattern, that is to say, the broadened glow-like plasma originating from the localized guided-streamer.

Accordingly, it has been demonstrated that the proposed APPJs, *i.e.*, three-array jets with GB system, can form a wide uniform glow-like plasma in order to uniformly process the entire area of the PET film. These results, as in our previous report, can be applied to applications where P-LEDs and gas sensor devices require a very smooth and thin film as a conductive or sensing material by plasma polymerization techniques [3], [43].

IV. CONCLUSION

In order to improve the capability of the uniform area-treatment for the conventional APPJs, we experimentally performed case studies depending on the variations of APPJ structures, such as the number of array jets and GB system including gas compositions. Only in case of three-array jets with GB system using Ar + O_2 gas, the intense glow-like plasma including abundant RNS ranging between 330 and 380 nm, and ROS at 777.4 and 844.6 nm, was produced. The abundant RNS and ROS were induced by adopting the GB system. In particular, in case of the three-array jets with GB system, the plasma-treated PET films showed a remarkable increase in oxygen-containing hydrophilic polar groups, such as, C-O/C-OH bonds, and a slight decrease of C-C/C-H bonds, as confirmed by the XPS analysis. In addition, the nitrogen bond of -N=O, directly resulting in the improvement of the surface hydrophilicity, was newly generated, as confirmed by the XPS analysis.

Furthermore, as confirmed by the WCA analysis with the lower CAa and CAsd values of the entire area (=10 mm × 10 mm) of PET substrate, the hydrophilic surface treatment can be effectively performed by the wide intense glow-like plasma generated by the proposed APPJs, *i.e.*, three-array jets with GB system. Therefore, it is expected that the proposed APPJs will contribute to enhancing the uniform surface treatment capability by overcoming the localized area treatment problem of the conventional APPJs.

REFERENCES

[1] D. A. G. Sawtell, Z. Abd-Allah, J. W. Bradley, G. T. West, and P. J. Kelly, ''Mechanisms of atmospheric pressure plasma treatment of BOPP,'' *Plasma Process. Polym.*, vol. 15, no. 1, Jan. 2017, Art. no. 1700051.

[2] A. van Deynse, R. Morent, C. Leys, and N. De Geyter, ''Influence of ethanol vapor addition on the surface modification of polyethylene in a dielectric barrier discharge,'' *Appl. Surf. Sci.*, vol. 419, pp. 847–859, Oct. 2017.

[3] C.-S. Park, D. Kim, B. Shin, D. Y. Kim, H.-K. Lee, and H.-S. Tae, ''Conductive polymer synthesis with single-crystallinity via a novel plasma polymerization technique for gas sensor applications,'' *Materials*, vol. 9, no. 10, p. 812, Oct. 2016.

[4] C.-S. Park, D. Kim, B. J. Shin, and H.-S. Tae, ''Synthesis and characterization of nanofibrous polyaniline thin film prepared by novel atmospheric pressure plasma polymerization technique,'' *Materials*, vol. 9, no. 1, p. 39, Jan. 2016.

[5] A. Kuzminova, T. Kretková, O. Kylián, J. Hanuš, I. Khalakhan, V. Prukner, E. Doležalová, M. Šimek, and H. Biederman, ''Etching of polymers, proteins and bacterial spores by atmospheric pressure DBD plasma in air,'' *J. Phys. D, Appl. Phys.*, vol. 50, no. 13, Feb. 2017, Art. no. 135201.

[6] P. Dimitrakellis, A. Travlos, V. P. Psycharis, and E. Gogolides, ''Superhydrophobic paper by facile and fast atmospheric pressure plasma etching,'' *Plasma Processes Polym.*, vol. 14, no. 3, Mar. 2017, Art. no. 1600069.

[7] B. F. Gilmore, P. B. Flynn, S. O'Brien, N. Hickok, T. Freeman, and P. Bourke, ''Cold plasmas for biofilm control: Opportunities and challenges,'' *Trends Biotechnol.*, vol. 36, no. 6, pp. 627–638, Jun. 2018.

[8] A. Sakudo, H. Miyagi, T. Horikawa, R. Yamashiro, and T. Misawa, ''Treatment of Helicobacter pylori with dielectric barrier discharge plasma causes UV induced damage to genomic DNA leading to cell death,'' *Chemosphere*, vol. 200, pp. 366–372, Jun. 2018.

[9] Y.-J. Zhou, Q.-H. Yuan, F. Li, X.-M. Wang, G.-Q. Yin, and C.-Z. Dong, ''Nonequilibrium atmospheric pressure plasma jet using a combination of 50 kHz/2 MHz dual-frequency power sources,'' *Phys. Plasmas*, vol. 20, no. 11, Oct. 2013, Art. no. 113502.

[10] U. Lommatzsch, D. Pasedag, A. Baalmann, G. Ellinghorst, and H.-E. Wagner, ''Atmospheric pressure plasma jet treatment of polyethylene surfaces for adhesion improvement,'' *Plasma Process. Polym.*, vol. 4, no. S1, pp. S1041–S1045, Apr. 2007.

[11] K. G. Doherty, J.-S. Oh, P. Unsworth, A. Bowfield, C. M. Sheridan, P. Weightman, J. W. Bradley, and R. L. Williams, ''Polystyrene surface modification for localized cell culture using a capillary dielectric barrier discharge atmospheric-pressure microplasma jet,'' *Plasma Process. Polym.*, vol. 10, no. 11, pp. 978–989, Nov. 2013.

[12] H. Jung, B. Gweon, D. B. Kim, and W. Choe, ''A simple approach to surface modification using polytetrafluoroethylene (PTFE) with laminar and turbulent flows of micro plasma jets at atmospheric pressure,'' *Plasma Process. Polym.*, vol. 8, no. 6, pp. 535–541, Jun. 2011.

[13] B. K. H. L. Boekema, M. Vlig, D. Guijt, K. Hijnen, S. Hofmann, P. Smits, A. Sobota, E. M. van Veldhuizen, P. Bruggeman, and E. Middelkoop, ''A new flexible DBD device for treating infected wounds: *In vitro* and *ex vivo* evaluation and comparison with a RF argon plasma jet,'' *J. Phys. D, Appl. Phys.*, vol. 49, no. 4, Dec. 2015, Art. no. 044001.

[14] P. Dimitrakellis, A. Zeniou, Y. Stratakos, and E. Gogolides, ''Radio frequency atmospheric plasma source on a printed circuit board for large area, uniform processing of polymeric materials,'' *Plasma Sources Sci. Technol.*, vol. 25, no. 2, Feb. 2016, Art. no. 025015.

[15] S.-O. Kim, J. Y. Kim, D. Y. Kim, and J. Ballato, ''Intense plasma emission induced by jet-to-jet coupling in atmospheric pressure plasma arrays,'' *Appl. Phys. Lett.*, vol. 101, no. 17, Oct. 2012, Art. no. 173503.

[16] J. Y. Kim, J. Ballato, and S.-O. Kim, ''Intense and energetic atmospheric pressure plasma jet arrays,'' *Plasma Process. Polym.*, vol. 9, no. 3, pp. 253–260, Mar. 2012.

[17] X. Lu, G. V. Naidis, M. Laroussi, and K. Ostrikov, ''Guided ionization waves: Theory and experiments,'' *Phys. Rep.*, vol. 540, no. 3, pp. 123–166, Jul. 2014.

[18] D. H. Kim, C.-S. Park, W. H. Kim, B. J. Shin, J. G. Hong, T. S. Park, J. H. Seo, and H.-S. Tae, ''Influences of guide-tube and bluff-body on advanced atmospheric pressure plasma source for single-crystalline polymer nanoparticle synthesis at low temperature,'' *Phys. Plasmas*, vol. 24, no. 2, Jan. 2017, Art. no. 023506.

[19] X. Lu, M. Laroussi, and V. Puech, ''On atmospheric-pressure non-equilibrium plasma jets and plasma bullets,'' *Plasma Sources Sci. Technol.*, vol. 21, no. 3, 2012, Art. no. 034005.

[20] U. Kogelschatz, ''Dielectric-barrier discharges: Their history, discharge physics, and industrial applications,'' *Plasma Chem. Plasma Process.*, vol. 23, no. 1, pp. 1–46, Mar. 2003.

[21] T. Shao, C. Zhang, R. Wang, Y. Zhou, Q. Xie, and Z. Fang, ''Comparison of atmospheric-pressure He and Ar plasma jets driven by microsecond pulses,'' *IEEE Trans. Plasma Sci.*, vol. 43, no. 3, pp. 726–732, Mar. 2015.

[22] X.-J. Shao, N. Jiang, G.-J. Zhang, and Z.-X. Cao, ''Comparative study on the atmospheric pressure plasma jets of helium and argon,'' *Appl. Phys. Lett.*, vol. 101, no. 25, Dec. 2012, Art. no. 253509.

[23] S. Wang, V. Schulz-Von der Gathen, and H. F. Döbele, ''Discharge comparison of nonequilibrium atmospheric pressure Ar/O_2 and He/O_2 plasma jets,'' *Appl. Phys. Lett.*, vol. 83, no. 16, pp. 3272–3274, Aug. 2003.

[24] Y. S. Seo, A.-A. H. Mohamed, K. C. Woo, H. W. Lee, J. K. Lee, and K. T. Kim, ''Comparative studies of atmospheric pressure plasma characteristics between He and Ar working gases for sterilization,'' *IEEE Trans. Plasma Sci.*, vol. 38, no. 10, pp. 2954–2962, Aug. 2010.

[25] W.-C. Zhu, Q. Li, X.-M. Zhu, and Y.-K. Pu, ''Characteristics of atmospheric pressure plasma jets emerging into ambient air and helium,'' *J. Phys. D, Appl. Phys.*, vol. 42, no. 20, Sep. 2009, Art. no. 202002.

[26] A. J. Knoll, P. Luan, E. A. J. Bartis, C. Hart, Y. Raitses, and G. S. Oehrlein, ''Real time characterization of polymer surface modifications by an atmospheric-pressure plasma jet: Electrically coupled versus remote mode,'' *Appl. Phys. Lett.*, vol. 105, no. 17, 2014, Art. no. 171601.

[27] Z. Fang, C. Ruan, T. Shao, and C. Zhang, ''Two discharge modes in an atmospheric pressure plasma jet array in argon,'' *Plasma Sources Sci. Technol.*, vol. 25, no. 1, Nov. 2015, Art. no. 01LT01.

[28] J. H. Kim, H.-J. Kim, J. Y. Kim, and H.-S. Tae, ''Intense ar plasma array jet with ring-type focusing electrode,'' *IEEE Trans. Plasma Sci.*, vol. 42, no. 10, pp. 2478–2479, Oct. 2014.

[29] D. B. Graves, ''The emerging role of reactive oxygen and nitrogen species in redox biology and some implications for plasma applications to medicine and biology,'' *J. Phys. D, Appl. Phys.*, vol. 45, no. 26, Jun. 2012, Art. no. 263001.

[30] Z. Machala, B. Tarabova, K. Hensel, E. Spetlikova, L. Sikurova, and P. Lukes, ''Formation of ROS and RNS in water electro-sprayed through transient spark discharge in air and their bactericidal effects,'' *Plasma Processes Polym.*, vol. 10, no. 7, pp. 649–659, 2013.

[31] A. El-Zein, M. Talaat, G. El-Aragi, and A. El-Amawy, ''Electrical characteristics of nonthermal gliding arc discharge reactor in argon and nitrogen gases,'' *IEEE Trans. Plasma Sci.*, vol. 44, no. 7, pp. 1155–1159, Jul. 2016.

[32] J. Y. Kim and S.-O. Kim, ''Intense plasma emission from atmospheric-pressure plasma jet array by jet-to-jet coupling,'' *IEEE Trans. Plasma Sci.*, vol. 39, no. 11, pp. 2278–2279, Nov. 2011.

[33] Z. Fang, H. Yang, and Y. Qiu, ''Surface treatment of polyethylene terephthalate films using a microsecond pulse homogeneous dielectric barrier discharges in atmospheric air,'' *IEEE Trans. Plasma Sci.*, vol. 38, no. 7, pp. 1615–1623, Jul. 2010.

[34] I. Novák, A. Popelka, A. S. Luyt, M. M. Chehimi, M. Špírková, I. Janigová, A. Kleinová, P. Stopka, M. Šlouf, V. Vanko, I. Chodák, and M. Valentin, ''Adhesive properties of polyester treated by cold plasma in oxygen and nitrogen atmospheres,'' *Surf. Coat. Technol.*, vol. 235, pp. 407–416, Nov. 2013.

[35] N. L. Singh, A. Qureshi, N. Shah, A. K. Rakshit, S. Mukherjee, A. Tripathi, and D. K. Avasthi, ''Surface modification of polyethylene terephthalate by plasma treatment,'' *Radiat. Meas.*, vol. 40, nos. 2–6, pp. 746–749, Nov. 2005.

[36] J. Ortiz-Medina, H. Kitano, A. Morelos-Gomez, Z. Wang, T. Araki, C.-S. Kang, T. Hayashi, K. Takeuchi, T. Kawaguchi, A. Tanioka, R. Cruz-Silva, M. Terrones, and M. Endo, ''Nanostructured carbon-based membranes: Nitrogen doping effects on reverse osmosis performance,'' *NPG Asia Mater.*, vol. 8, no. 4, Apr. 2016, Art. no. e258.

[37] Z. Zheng, L. Ren, W. Feng, Z. Zhai, and Y. Wang, ''Surface characterization of polyethylene terephthalate films treated by ammonia low-temperature plasma,'' *Appl. Surf. Sci.*, vol. 258, no. 18, pp. 7207–7212, Jul. 2012.

[38] Z. Zheng, L. Ren, Z. Zhai, Y. Wang, and F. Hang, "Surface modification on polyethylene terephthalate films with 2-methacryloyloxyethyl phosphorylcholine," *Mater. Sci. Eng., C*, vol. 33, no. 5, pp. 3041–3046, Jul. 2013.

[39] J. Lei, L. Yang, Y. Zhan, Y. Wang, T. Ye, Y. Li, H. Deng, and B. Li, "Plasma treated polyethylene terephthalate/polypropylene films assembled with chitosan and various preservatives for antimicrobial food packaging," *Colloids Surf., Biointerfaces*, vol. 114, pp. 60–66, Feb. 2014.

[40] K. G. Kostov, T. M. C. Nishime, A. H. R. Castro, A. Toth, and L. R. O. Hein, "Surface modification of polymeric materials by cold atmospheric plasma jet," *Appl. Surf. Sci.*, vol. 314, pp. 367–375, Sep. 2014.

[41] M.-J. Chuang and A.-K. Chu, "Formation of a high hydrophilic/hydrophobic contrast surface on PET substrates by ECR generated sulfur hexafluoride plasma," *Appl. Surf. Sci.*, vol. 257, no. 9, pp. 3943–3947, Feb. 2011.

[42] O. T. Olabanji and J. W. Bradley, "Side-on surface modification of polystyrene with an atmospheric pressure microplasma jet," *Plasma Process. Polym.*, vol. 9, no. 9, pp. 929–936, Sep. 2012.

[43] C.-S. Park, D. Y. Kim, D. H. Kim, H.-K. Lee, B. J. Shin, and H.-S. Tae, "Humidity-independent conducting polyaniline films synthesized using advanced atmospheric pressure plasma polymerization with *in-situ* iodine doping," *Appl. Phys. Lett.*, vol. 110, no. 3, Jan. 2017, Art. no. 033502.

DONG HA KIM received the B.S. and M.S. degrees from the School of Electronics Engineering, College of IT, Kyungpook National University, Daegu, South Korea, in 2013 and 2015, respectively, where he is currently pursuing the Ph.D. degree in electronic and electrical engineering. He is also a Postdoctoral with the Korea Institute of Industrial Technology (KITECH), Ulsan, South Korea. His research interests include physics of surface treatment, removing volatile organic compounds (VOC), recycling of plastic waste, and plasma polymerization using atmospheric pressure plasma jet (APPJ).

CHOON-SANG PARK received the M.S. and Ph.D. degrees in electronic and electrical engineering from Kyungpook National University, Daegu, South Korea, in 2006 and 2010, respectively, where he was a Senior Researcher/Research Professor with the School of Electrical Engineering and Computer Science, from 2010 to 2019. He was also a Postdoctoral Fellow with Clemson University, Clemson, SC, USA. He is currently a Research Professor with the Digital Technology Research Center (DTRC), Kyungpook National University. His research interests include microplasma, atmospheric pressure plasma, fluid dynamics, plasma polymerization, plasma physics, and plasma chemistry.

BHUM JAE SHIN received the B.S., M.S., and Ph.D. degrees in plasma engineering from Seoul National University, Seoul, South Korea, in 1990, 1992, and 1997, respectively. From 1997 to 2000, he was a Senior Researcher with the PDP Team, Samsung SDI, Cheonan, South Korea. From 2000 to 2001, he was a Visiting Researcher with the Physics Department, Stevens Institute of Technology, Hoboken, NJ, USA. Since 2003, he has been a Professor with the Department of Electronics Engineering, Sejong University.

JEONG HYUN SEO received the B.S., M.S., and Ph.D. degrees in plasma engineering from Seoul National University, Seoul, South Korea, in 1993, 1995, and 2000, respectively. He was with Plasma Display Panel (PDP) Division, Samsung SDI, Cheonan, South Korea, from 2000 to 2002, where his work focused on the design of driving pulse in ac PDP. Since September 2002, he has been a Professor with the Department of Electronics Engineering, University of Incheon, Incheon, South Korea. He is currently a member of the Society for Information Display (SID) and the Korean Information Display Society.

HEUNG-SIK TAE (M'00–SM'05) received the B.S., M.S., and Ph.D. degrees in electrical engineering from Seoul National University, Seoul, South Korea, in 1986, 1988, and 1994, respectively. He had been a Consulting Professor for the Samsung SDI for six years, from 2004 to 2009. He had been a Research Head of the PDP Division with the Korean Information Display Society (KIDS). Since 1995, he has been a Professor with the School of Electronics Engineering, College of IT, Kyungpook National University, Daegu, South Korea. His research interests include atmospheric pressure plasma, solution plasma process, liquid plasma process, plasma polymerization, and flexible display devices, such as PLED. Since 2005, he has been serving as an Editor for the IEEE TRANSACTIONS ON ELECTRON DEVICES section on display technology for nine years. He has been the Director of the BK21 PLUS KNU ICT Research Center, since 2013.